

# Experimental Investigation of Lubrication Properties at High Contact Pressure

Huaping Xiao · Dan Guo · Shuhai Liu ·  
Xinchun Lu · Jianbin Luo

Received: 14 March 2010 / Accepted: 8 June 2010 / Published online: 24 June 2010  
© Springer Science+Business Media, LLC 2010

**Abstract** A new test rig with an ability to obtain clear interference images at high pressure contacts has been developed. The technique of relative optical interference intensity has been used to obtain film thickness profiles and then lubrication properties of some base oils including six kinds of polyalphaolefin and four kinds of silicone oil have been studied at different pressures ranging from 1 to 3 GPa. The results show that viscosities of these lubricants have notable effect on slopes of film thickness curves (speed versus film thickness in log–log form), and the observed phenomenon is attributed to fluidity and molecular structure. A comparison of experimental central film thicknesses with computational work shows that at high loads the relationship between load and film thickness usually go against prediction given by Hamrock and Dowson. In addition, when more pressure is applied, the profiles of film thickness become more and more flat while rolling speed do little to change the shape of profiles.

**Keywords** High contact pressure ·  
Elastohydrodynamic lubrication · Thin film lubrication ·  
Lubrication properties · Base oil

---

H. Xiao · D. Guo (✉) · X. Lu · J. Luo  
State Key Laboratory of Tribology, Tsinghua University, Beijing  
100084, People's Republic of China  
e-mail: guodan26@mail.tsinghua.edu.cn

H. Xiao  
e-mail: xiaohuaping107@yahoo.cn

S. Liu  
School of Mechanical and Electronic Engineering, China  
University of Petroleum, Beijing 102249,  
People's Republic of China

## 1 Introduction

For a long period, the study in tribology has mainly focused on two fields, fluid lubrication and boundary lubrication. In fluid lubrication research, classical experimental and theoretical studies established the initial understanding of fluid film lubrication in 1880s. The publication of Reynolds equation in 1886 represented a milestone in the development of tribology. Since then, impressive developments in both analytic and experimental study in the field of hydrodynamic lubrication had been observed till another key concept in tribology was put forward. The birth of elastohydrodynamic lubrication (EHL) took place in the 1940s, and the study of mechanism of EHL is regarded as the major event in the development of tribology during the second half of last century. In 1949, Grubin found an approximate numerical solution to the EHL line contact problem, and his study was followed by the numerical solutions of the line contact given by Dowson and Higginson [1] in the late 1950s. In 1970s, Hamrock and Dowson [2] published a series of articles contributing to the complete solution of numerical problem for more general point contacts, and EHL has been greatly developed by many authors both theoretically and experimentally at the end of the twentieth century.

In boundary lubrication research, initial study by Hardy [3] established in 1922 that the coefficient of friction is influenced by the nature of the rubbing bodies and by the molecular structure of the lubricant, and his model gained supremacy over other alternatives over a long time. Other models and studies being aimed at improving the understanding about the principle of boundary lubrication and the failure of lubricant film were gradually developed by Bowden and Tabor [4], Adamson [5], Kingsbury [6], Sharma and Cameron [7], Homola et al. [8], Luo et al. [9], and others.

Up till now, the gap between fluid lubrication and boundary lubrication has been largely decreased by the establishment of mixed lubrication theory [10, 11] and micro-EHL theory [12]. A number of equations have been set up and are widely used to calculate film thickness under different situations.

Most of the researchers focused their attention on the study at low and moderate contact pressures below approximately 1 GPa. However, high contact pressures up to 2 GPa or even 3 GPa are found in practicing conditions such as in cams, gears, and rolling bearings. Therefore, the issue that whether those equations in common use derived at low and moderate pressures are still valid at the conditions of high pressures has been concerned by a great number of researchers for a long time. The main barrier to solve this problem is that appropriate experimental instruments for high pressures are not easily accessible. Initial study, attempting to discover how film thickness is influenced by various factors such as the properties of the lubricants, temperature, speed, and load, by Lane and Hughes [13] in 1950s, applied electrical contact resistance method, but accurate value of film thickness was not determined. In early 1960s, the development of optical interferometry technique [14] makes it possible to confirm the theoretical film thickness predicted by classical equations. This technique has been widely used in the research of lubrication films today. In 1960s and 1970s, the approach of the optical interferometry technique, which was used in conjunction with ball-on-disk apparatus for measuring lubricant film thickness, had been applied and gradually consolidated. Currently, there are numerous variants [9, 15, 16] of this approach developed by research groups all over the world. Unfortunately, most of these instruments can only conduct measurement of film thickness at low and moderate pressures. Study on extreme conditions is still at the initial stage.

Numerical study by Zhu [17, 18] suggested that the classical formula given by Hamrock and Dowson may be invalid at very high contact pressures in starvation condition. Smeeth and Spikes [19] obtained central and minimum elastohydrodynamic film thicknesses at very high contact pressure up to 3.5 GPa using a tungsten carbide ball. Krupka et al. [20] studied thin lubricating films behavior at high pressure up to 3 GPa also using a tungsten carbide ball against sapphire disk. Although these results do shed light on lubrication properties of lubricants at very high contact pressure, there are some limitations. Smeeth only focused on elastohydrodynamic films with thickness above 100 nm, and Krupka's study is confined to discuss film thickness in thin film lubrication conditions. They employed tungsten carbide ball in their study, while steel ball is most commonly used in operating situations. In

addition, they only used a small amount of lubricants in the research, and so a general rule cannot be summarized.

This research article on the lubrication properties of a series of base oils at very high contact pressure up to 3 GPa in detail. In order to get more reliable datum, a new test instrument for measuring film thickness at high pressures is developed to study performance of lubricants in practical situations. Lubricating films formed by these base oils are directly measured, employing relative optical interference intensity method [9, 21]. Results of different base oils are compared at a range of contact pressure from 1 to 3 GPa. This article is aimed at finding out the effect of high pressure on the film thickness for several fluids and examining whether the classical EHL theory and equations are still valid at extreme conditions.

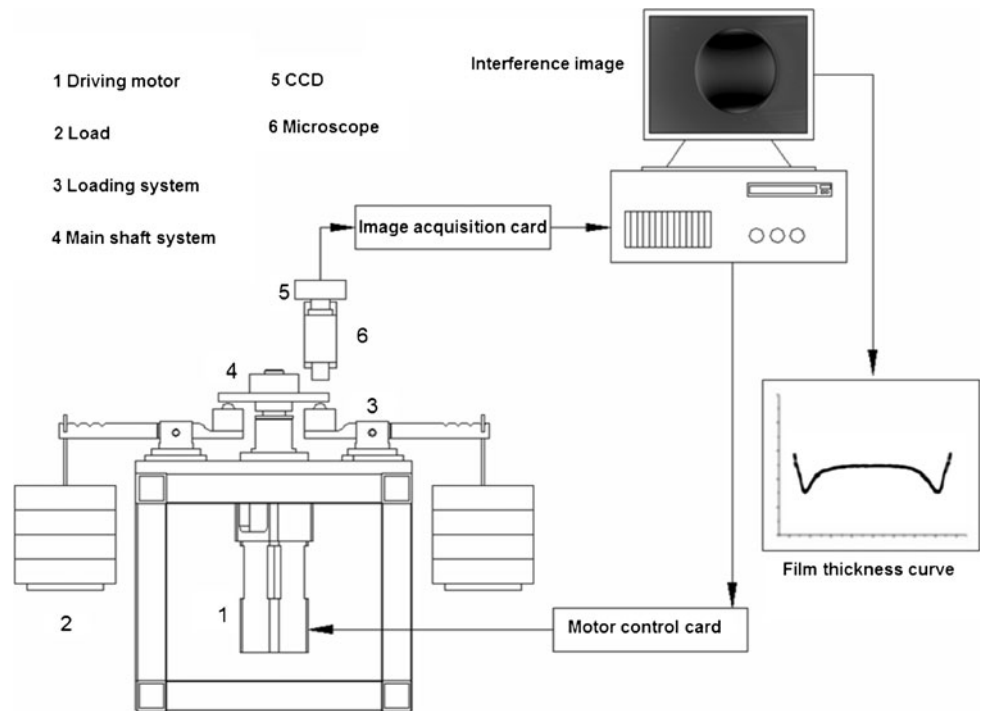
## 2 Approaches and Methods

### 2.1 Test Instrument

Film thicknesses of lubricants are measured on real-time basis employing the technique of relative optical interference intensity. In order to obtain clear images and more accurate data, a new test rig is used in these experiments. The schematic representation of the new film measuring system is shown in Fig. 1. When a load is applied, a contact is formed between the surface of sapphire disk coated with a semireflective layer of chromium and the surface of steel ball with diameter of 12.7 mm. When the monochromatic light whose wavelength is about 600 nm is shone into the contact area, part of the light is reflected from the chromium layer, while some passes through the lubricant film and is reflected from the steel ball. Then, the two reflected beams separately recombine and interfere. The monochromatic interference fringe is then captured by a CCD which translates optical signal into electrical signal after the beams passes through a microscope. The electrical signal is processed by image acquisition card and the image of contact is then presented in the screen of computer. Finally, information of film thickness is obtained through a treatment of these images.

The mechanical structure is designed to be suitable for test at very high contact pressures. The sapphire disk is driven by a motor through a main shaft and a flexible coupling. Steel ball is loaded against the disk and gets located in a small chamber. The disk is driven to rotate and which, in turn, drives the ball in pure rolling. In this test rig, balancing as well as loading mechanisms are used to reduce bending moment applied to the main shaft. If the main shaft is affected by bending moment for a long time, then a bending deformation may take place, which leads to inaccuracy of data acquired. Therefore, the balancing

**Fig. 1** Schematic representation of film measuring system



mechanism can ensure the stability and rotating accuracy of the main shaft, and prolong its service life. Rotating speed of sapphire disk is controlled by computer so that experiments can be operated in a series of speeds.

### 2.2 Principle of Relative Optical Interference Intensity

The principle of relative optical interference intensity method is shown in Fig. 2 and briefly described later. The vertical resolution of this measurement method is 0.5 nm, and the horizontal resolution is 1.4 μm. More details can be seen in [9, 21]. The basic equation of optical interference under vertical incidence light is expressed as

$$I = I_1 + I_2 + 2\sqrt{I_1 I_2} \cos(4nh\pi/\lambda + \phi) \quad (1)$$

where  $I$  is the interference intensity at the measured point;  $I_1$  and  $I_2$  are the intensities of beam 1 and beam 2, respectively, as shown in Fig. 2.  $n$  is the refractive index of

the lubricant, and  $\lambda$  is the wavelength of the incidence light which is about 600 nm.  $4nh\pi/\lambda + \phi$  is the phase difference. Then, film thickness  $h$  can be expressed as

$$h = \frac{\lambda}{4\pi n} [\arccos(\bar{I}) - \phi] \quad (2)$$

where  $\bar{I}$  is defined as the relative intensity and can be expressed as

$$\bar{I} = \frac{2I - (I_{\max} + I_{\min})}{I_{\max} - I_{\min}} \quad (3)$$

where  $I_{\max}$  and  $I_{\min}$  are the maximum and minimum intensities, respectively. When film thickness is zero, the relative intensity is defined as  $\bar{I}_0$ , and  $\phi$  equals to  $\arccos(\bar{I}_0)$  from Eq. 2. Therefore, the final expression of  $h$  is

$$h = \frac{\lambda}{4\pi n} [\arccos(\bar{I}) - \arccos(\bar{I}_0)] \quad (4)$$

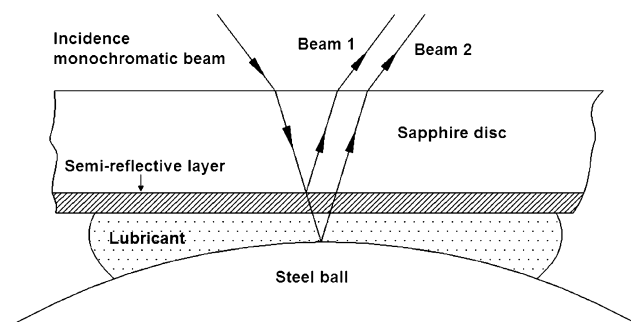


**Fig. 2** Principal sketch of optical interference intensity

### 2.3 Materials and Methods

In this study, film thicknesses between the steel ball and the sapphire disk were measured at high pressure up to 3 GPa at room temperature. Six kinds of polyalphaolefin (PAO) (PAO 2, 4, 5, 7, 8, and 9) and four kinds of silicone oils (silicone oil 300, 500, 700, and 1000) are used. They were selected on the basis that they are base oils in common use with different viscosities and that they separately represent Newtonian fluid and non-Newtonian fluid. Therefore, the results of this experiment can not only reveal how base oils

perform at high pressure, but also can compare different features of them.

A sapphire disk of 20-mm thickness and a diameter of 140 mm is used for the reason that only thick sapphire disk can meet the requirement of transparency and be able to resist high pressures up to 2–3 GPa. In order to ensure the clarity of the images acquired, instead of tungsten carbide ball, we selected commercial steel ball of 5 nm root mean square surface roughness offered by NSK CORP.

#### 2.4 Influence of Pressure on Refractive Index

In order to obtain value of film thickness, it is necessary to know the refractive index of the lubricants at different pressures. In this study, the refractive indexes of the oils were measured at atmospheric pressure using Abbe refractometer.

In order to obtain the refractive index under different pressures, we need to know the refractive index–density correlation of these oils. However, the elasto-optical behavior of liquids at high pressure cannot be exactly predicted by any of the current prevalent equation [22]. However, if the error is limited to an acceptable scale, then we think it is reasonable to use a certain equation. In this study, we employ Lorentz–Lorenz equation [23] to predict density–refractive index relationship, and use the formula given by Dowson and Higginson [24] to predict pressure–density relationship. The two formulas are chosen because the parameters needed to get the final result can be easily obtained, and the error is limited. The analysis about the error shows that under recent experimental situations the maximal error would only be 5.6%. The Lorentz–Lorenz equation is expressed as

$$\left(\frac{n^2 - 1}{n^2 + 1}\right) \frac{1}{\rho} = m \quad (5)$$

where  $n$  represents the refractive index at a specific pressure,  $\rho$  is the density of the lubricant, and  $m$  is a constant. Therefore,  $n$  can be expressed as

$$n = \left(\frac{1 + \rho m}{1 - \rho m}\right)^{1/2} \quad (6)$$

The value of  $m$  can be determined by the value of refractive index and density,  $n_0$  and  $\rho_0$ , respectively, measured at atmosphere pressure. Furthermore, the density of lubricants can be described by the following relationship obtained from Dowson and Higginson:

$$\frac{\rho}{\rho_0} = 1 + \frac{0.6p}{(1 + 1.7p)} \quad (7)$$

where  $p$  is the pressure expressed in gigapascals. Using Eq. 7, the final expression of  $n$  can be written as

$$n = \left(\frac{1 + AB}{1 - AB}\right)^{1/2} \quad (8)$$

where  $A = \left(\frac{n_0^2 - 1}{n_0^2 + 1}\right)$  and  $B = 1 + \frac{0.6p}{1 + 1.7p}$ .

The estimated values of refractive index of all the 10 lubricants with increasing pressures are shown in Fig. 3. In this study, the film thicknesses at different pressures are measured using the calculated values of refractive index. It would yield an adequate approximation for this study.

### 3 Results and Discussion

#### 3.1 Observed Interference Image

Figure 4 shows the interference images of PAO 9 and silicone oil 300 at different conditions. The increase of contact area with growing pressure can be easily observed. As the rolling speed gradually rises, the outlet zone gets more and more obvious. It can be seen that the brightness of the central parts of these interference images at lower pressures change faster than that at higher pressures, which indicates that change of film thickness is much greater at lower pressures than at higher pressures.

#### 3.2 Feature of Film Thickness Curve

Figures 5 and 7 separately present the results of film thickness of PAO and silicone oil at different contact pressures and rolling speeds. The relationship between rolling speed and central film thickness is shown in the traditional log–log form. It can give a clear view of how the two series of oils perform at different conditions and demonstrate the influence of contact pressure and rolling speed on film-forming properties of these lubricants.

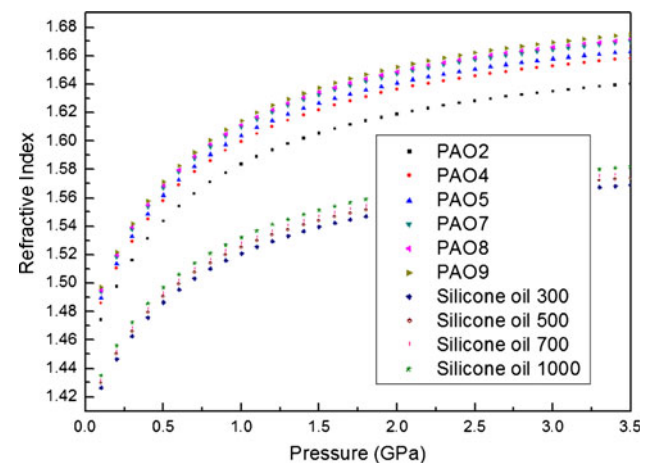


**Fig. 3** Numerical results of refractive index for the lubricants used

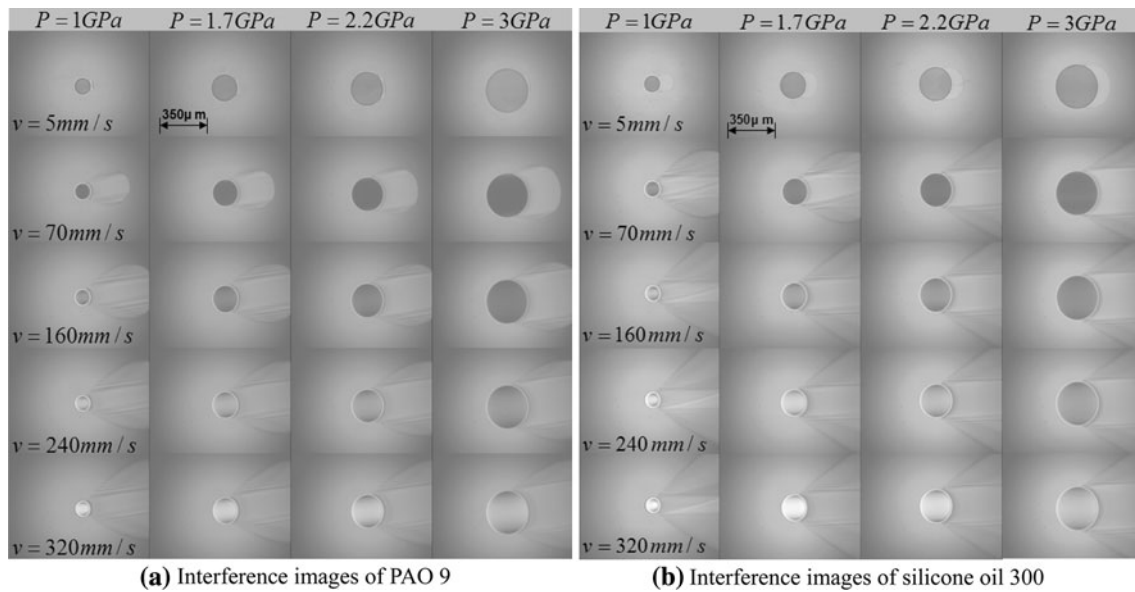


**Fig. 4** Interference images at different pressures and rolling speeds for PAO 9 and silicone oil 300

It can be clearly noted from Figs. 5 and 7 that speed indexes (the slopes of film thickness curves) vary with change of both rolling speed and applied pressure. All these plots are divided into several regions on the basis that, in every single region, speed index of a specific film thickness curve is roughly stable, and it differs from the speed index of the same film thickness curve in adjacent regions. The starting and the ending points of each region are determined by the observed variation of speed index.

In each region, the slopes of the fitting lines of film thickness curves are measured, and the values are used as speed indexes. Figures 6 and 8 show the relationship between viscosities and measured speed indexes at different pressures for PAO and silicone oils.

### 3.2.1 Variation of Speed Index for PAO

Figure 5 shows the measured film thickness of six kinds of PAO at different rolling speeds at four pressures, 1, 1.7, 2.2, and 3 GPa. It can be easily observed that the speed indexes of film thickness curves change with variations of both pressure and speed. The expression of relationship between film thickness and speed can be written as [9]

$$h = ku^\alpha \quad (9)$$

where  $h$  is the central film thickness,  $u$  is rolling speed,  $k$  is a coefficient related to the contact pressure and the properties of the frictional pair and lubricant, and  $\alpha$  is the speed index. According to classical formula suggested by Hamrock and Dowson, speed index is a constant in EHL.

Before the analysis of speed index, some points should be noted. Despite the fact that the film thickness curves of

the six PAO differ from each other, they can be divided into three groups for the reason that some curves share similar tendency and close speed index. Based on experimental results in this study, PAO 7, 8, and 9 compose a group, PAO 4 and 5 form a group, and PAO 2 by itself is a group. The stripes are used to distinct these groups at different regions. The viscosity of each lubricant and the average viscosity of the three different groups of PAO at atmospheric pressure and room temperature are listed in Table 1.

In Fig. 5a–c, the plots are divided into three regions, and in Fig. 5d, the plot is divided into two regions according to different speed indexes. It can be seen that in the region A, rolling speed and film thickness are relatively high, and lubrication state is EHL. In this region, the lubricating film is mainly composed of dynamic liquid film. Film thicknesses rise linearly with increasing rolling speed in log–log form, and thickness curves basically obey fitting lines, and thus the speed indexes are almost constants in this region. As rolling speed reduces, the film thickness curves do not conform to fitting lines in the region A any more. Speed indexes become either greater or smaller for different conditions, and the region, where film thickness curves lie, turns to the region B or the region C. In the region C, the lubrication state is failure of liquid lubrication (FLL, which means that in this state the lubrication film primarily consists of adsorbed film or static film, and film thickness rapidly gets down with further decreasing rolling speed). The speed indexes in the region C are normally greater than those in the region A, which can be observed in Fig. 5. The region B is a transition region, and the situation is rather complicated in this region. In this study, the regions A and C are analyzed in detail.

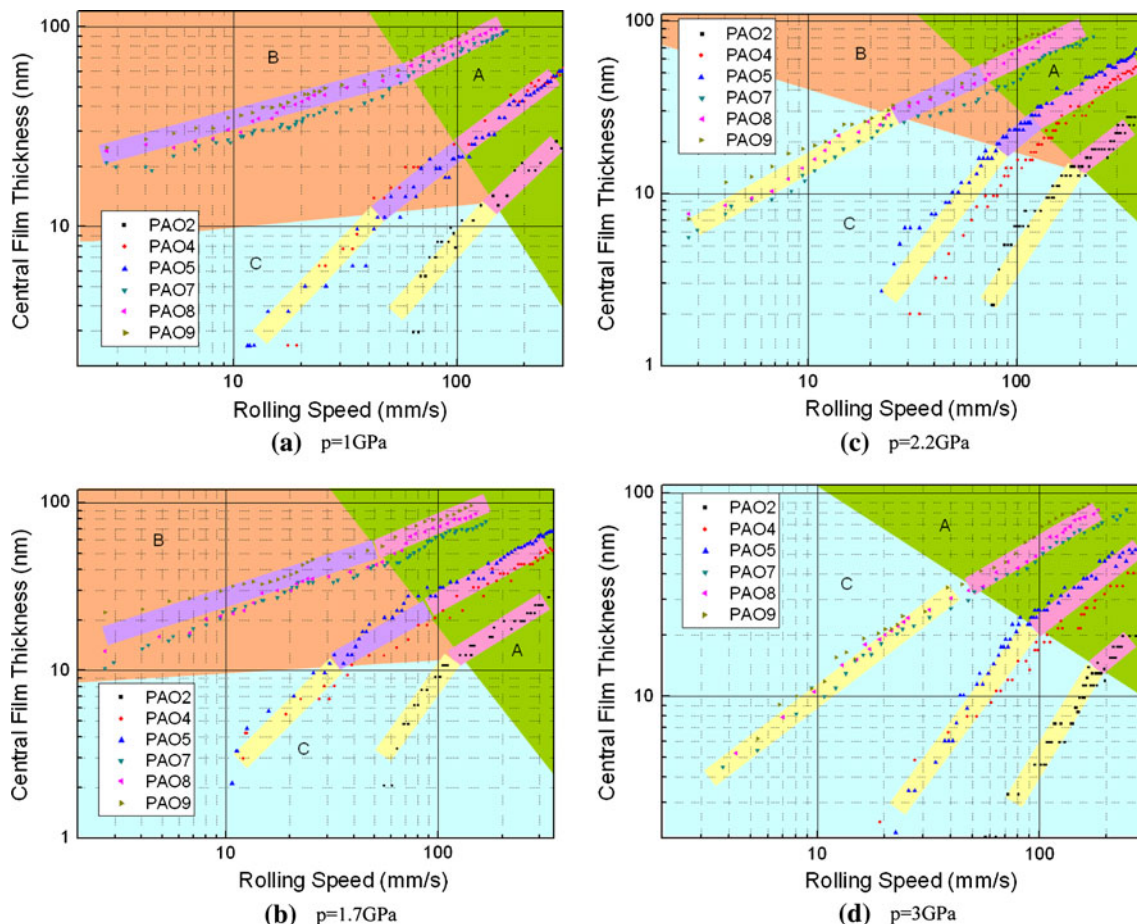


**Fig. 5** Central film thickness of PAO obtained at moderate and high pressure

In previous studies, most researchers focused their attention on how the slopes of film thickness curve change with rolling speed. However, in this study, the change tendency of speed index with viscosity and pressure is analyzed, and a number of features are of interest. The relationship between viscosities and measured speed indexes from curve fitting at different pressures for PAO is shown in Fig. 6. The viscosities and speed indexes used are the averaged values of the components of each group.

It can be seen from Fig. 6a that in the region A, the impact of pressure on speed index is limited. For each group, the difference between the maximum and minimum value of speed is 0.07 at most. No evident tendency of reduce or increase of speed index with pressure is observed. However, speed indexes do reduce as viscosity increases. In the region A, the greater the speed index is the faster the central film thickness increases with growing speed.

In the region C, the situation is somewhat different. The decreasing speed index with rising viscosity can also be seen in Fig. 6b. The phenomenon of interest is that for group 2 (PAO 4 and 5) and group 1 (PAO 2) speed index

rises as pressure increases. In this region, the bigger speed index means that when rolling speed gets down film thickness reduces more rapidly than else.

### 3.2.2 Variation of Speed Index for Silicone Oils

Figure 7 exhibits how the used four silicone oils perform at rolling speed ranging from 2 to 200 mm/s and at four different contact pressures, 1, 1.7, 2.2, and 3 GPa. Despite the fact that viscosities of the four silicone oils are distinct from each other, they share close tendency at all the four pressures. On the basis of these results, the four lubricants can be considered as belonging to the same group, and each plot is divided into parts according to the turns of film thickness curves. In order to obtain more insight into the lubrication properties of these silicone oils, speed indexes of film thickness curves resulting from fitting lines in regions A and C are also measured and shown in the form of speed index versus viscosity in Fig. 8.

It can be observed in Fig. 7 that at pressures of 1, 1.7, and 2.2 GPa, each film thickness curve is composed of three sections, and at 3 GPa, they are only divided into two

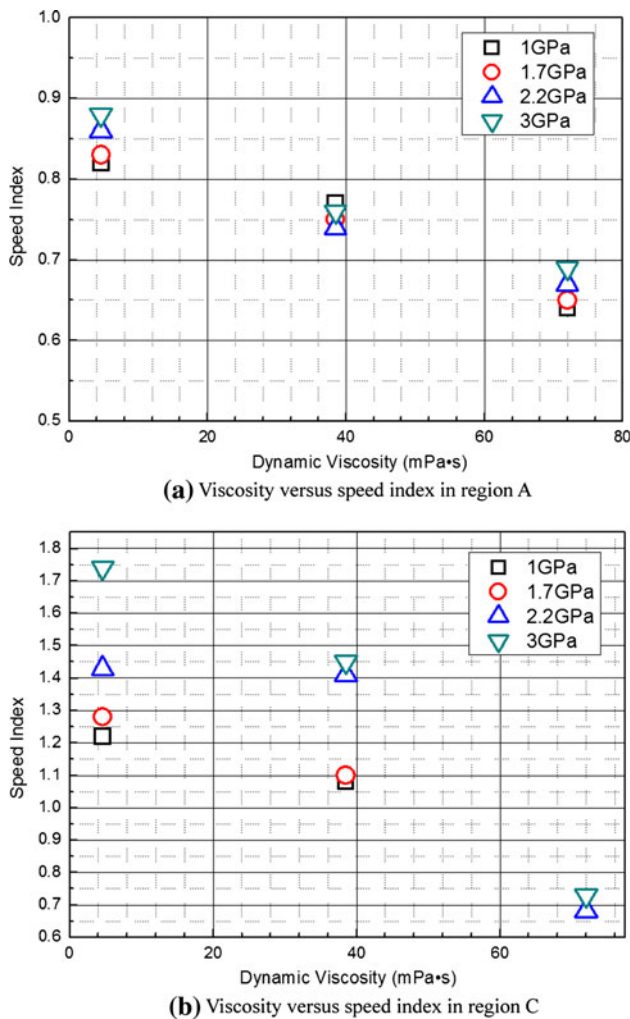


**Fig. 6** Relationship between viscosity and speed index at different pressures for PAO

major parts. In addition, it can be detected in Fig. 7 that the speed indexes in the region B are less than those in the regions A and C. Figure 8 shows that, like the situation for PAO, speed indexes in the region C are greater than those

in the region A. However, discrepancy can also be observed. In the region A, most speed indexes range from 0.5 to 0.6 regardless of different viscosities and pressures. In the region C, the relationship between speed index and pressure observed for PAO cannot be seen, and there is only a slight reduction of speed index with increasing viscosity compared to the phenomenon for PAO. The results indicate that speed index is related to viscosity to different extents for PAO and silicone oils. However, how does this happen?

In the region A, the film thickness–speed dependence is mainly determined by the lubricant flow and hydrodynamic action. For PAO, speed index reduces as viscosity increases, while speed index of silicone oil changes little when viscosity rises. Fluidity can be used to explain this behavior. The higher the fluidity of the liquid is, the more sensitive it is to speed, and fluidity obviously decreases as viscosity gets greater. Therefore, the speed index decreases when viscosity slowly increases as indicated by the observed results for PAO. However, as viscosity exceeds a certain value, the fluidity does not change much with further increase of viscosity. Therefore, speed indexes of silicone oils are roughly stable.

In the region C, fluid film is not the main portion of lubrication film any more. The use of lubricant flow and hydrodynamic action is not suitable for analysis of the results. In this study, molecular force and length of molecular chain are taken into account. When lubrication film is primarily composed of adsorbed film or static film, the film is formed taking advantage of molecular force. PAO and silicone oil are both polymers, and the lengths of their molecular chains vary for different kinds lubricants. Viscosity accordingly increases as molecular chain lengthens, and the molecular force rises. At low speed region, when speed gradually reduces, lubricant molecules are squeezed out of contact area. During this process, if the molecular force is larger, then it would be harder to squeeze out these molecules. Therefore, the lubricants with greater viscosity and more molecular force are less

**Table 1** Viscosity of all the lubricants at atmospheric pressure and room temperature

Lubricant	Viscosity (mPa s)	Average viscosity (mPa s)	Group (in Figs. 5, 6)
PAO 2	4.5	4.5	1
PAO 4	31	38	2
PAO 5	45		
PAO 7	56	71.7	3
PAO 8	74		
PAO 9	85		
Lubricant	Viscosity (mPa s)	Lubricant	Viscosity (mPa s)
Silicone oil 300	340	Silicone oil 500	490
Silicone oil 700	775	Silicone oil 900	975

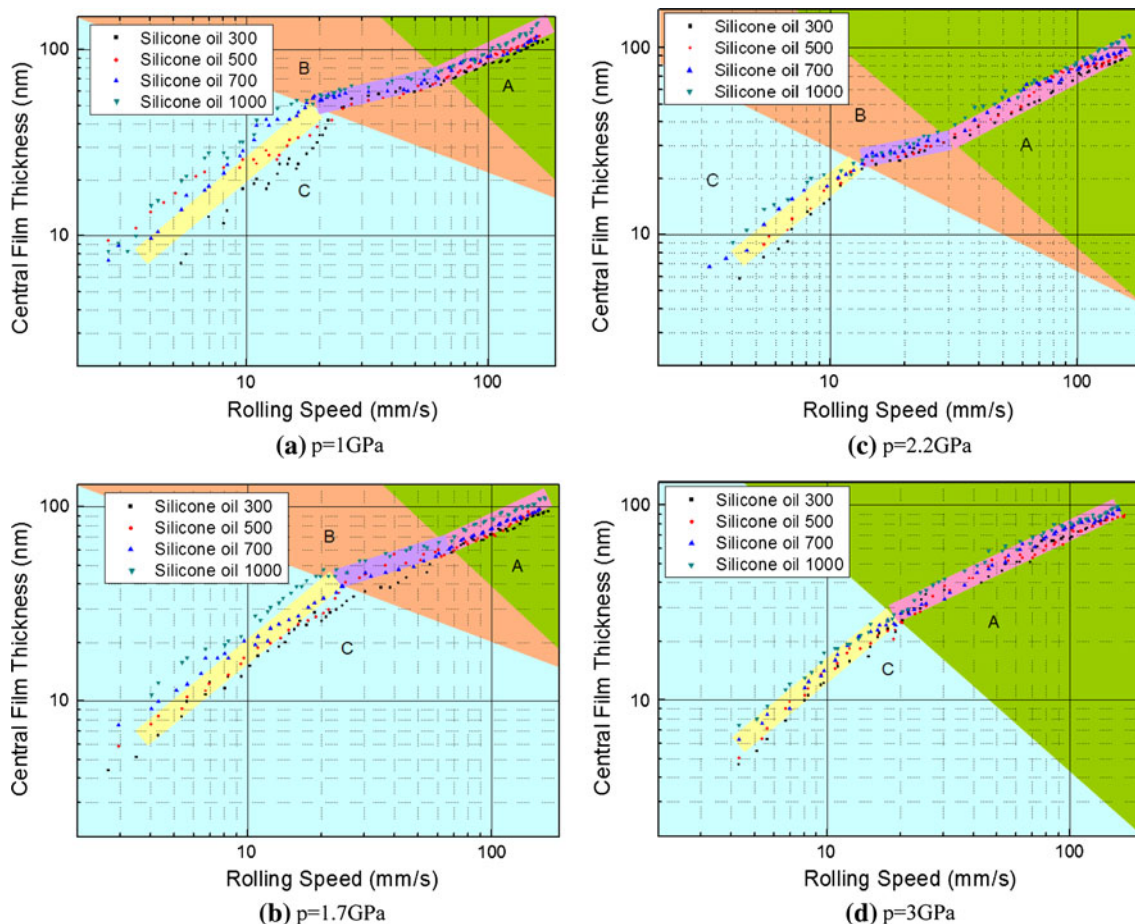


**Fig. 7** Central film thickness of silicone oil obtained at moderate and high pressures

sensitive to change of speed and have less speed indexes. When length of molecular chain overruns a certain value, molecular force changes little with further increase of viscosity. Therefore, the speed indexes of silicone oils reduce in a very limited extent as viscosities increase.

The effect of applied load on film thickness is discussed in the next section employing classical Hamrock–Dowson formula. Only some results of PAO are presented for the reason that this formula is not suitable for silicone oil.

### 3.3 Relationship Between Loads and Central Film Thicknesses

Figure 9 displays the relationship between the applied loads and central film thicknesses in log–log form for PAO 7, 8, and 9 at the speed of 100 mm/s. This plot shows both the predicted film thicknesses suggested by Hamrock and Dowson and the measured values for the three oils. The result is of considerable interest.

It can be clearly observed that, for PAO 7 at low and moderate loads, the measured values are very close to the

predicted ones. However, with increasing load, the measured film thicknesses decrease much faster than the computed ones. When load reaches 248 N where the contact pressure is 3 GPa, the measured amounts are much lower than the amounts of prediction.

The similar condition was observed for PAO 8. When the applied loads are 1.2, 9, and 45 N, corresponding to pressures of 0.5, 1, and 1.7 GPa, measurements and computed values are roughly equal, and then the measured film thickness drops more rapidly with increasing load. However, the results from PAO 9 indicate a reverse situation. The experimentally measured film thickness reduction is slower with increasing load compared to that predicted by the classical formula.

The experimental central film thickness dependence on pressure can be expressed as  $h \propto W^x$ , where  $W$  is the load applied.  $x$  equals to  $-0.11$ ,  $-0.08$ , and  $-0.061$  for PAO 7, 8 and 9, respectively. As opposed to the results found in this study, the  $x$  given by Hamrock and Dowson is  $-0.067$ .

The different values of  $x$  can be explained in terms of compressibility which means that as the fluid is



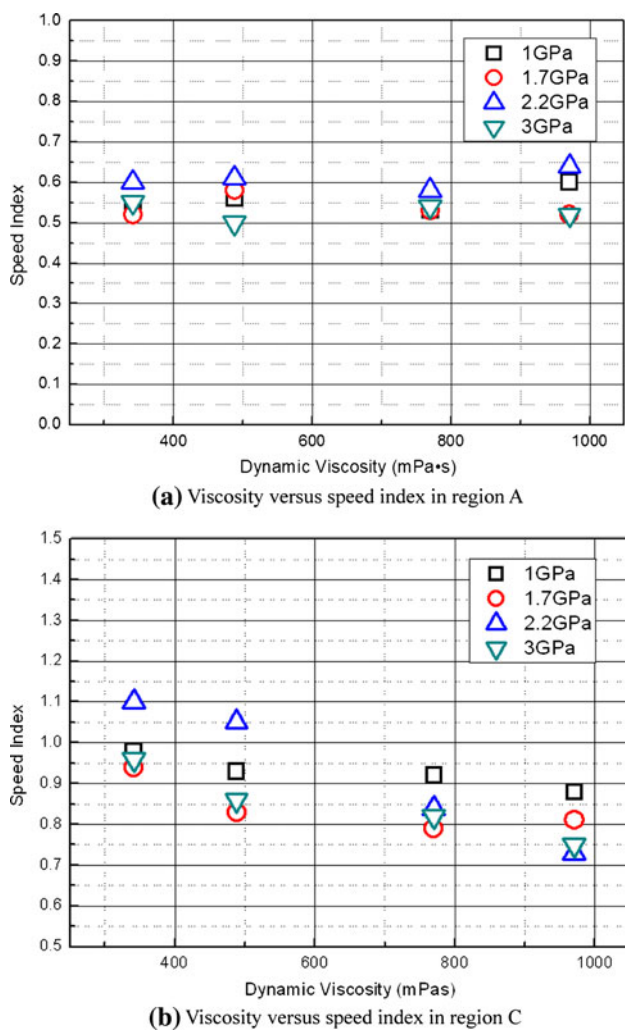


Fig. 8 Relationship between viscosity and speed index at different pressures for silicone oils

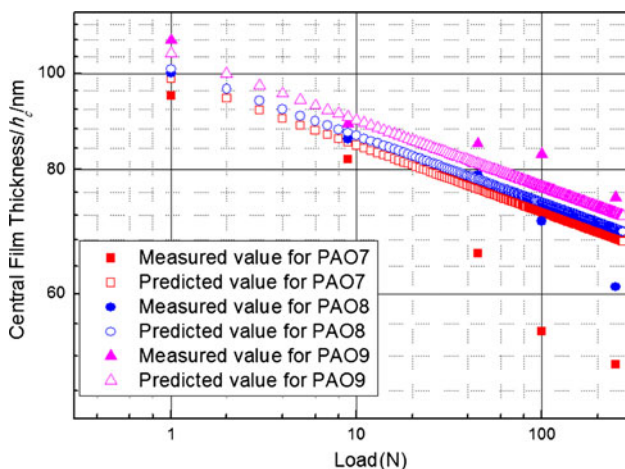


Fig. 9 Comparison of measured central film thickness/pressure dependence computational work

compressed, the distance between molecules gets smaller and smaller. The viscosities of PAO 7, 8, and 9 are different from each other, and PAO 7 and 9 separately have the lowest and highest viscosity, respectively. In addition, the three lubricants share similar molecular structure. Therefore, it can be inferred that compressibility of PAO 9 is the worst, and that of PAO 7 is the best. That is why when contact pressure gradually increases, the film thickness of PAO 7 decreases more rapidly than PAO 8 and 9.

In fact, the classical Hamrock–Dowson formula that resulted from the experiments operated mainly at low and moderate pressures. Therefore, when contact pressure gets very high and lubrication film is thin, the validity of classical EHL theory may become questionable. Similar conclusions have also been drawn by other authors [17, 19, 20] from their experimental or computed results.

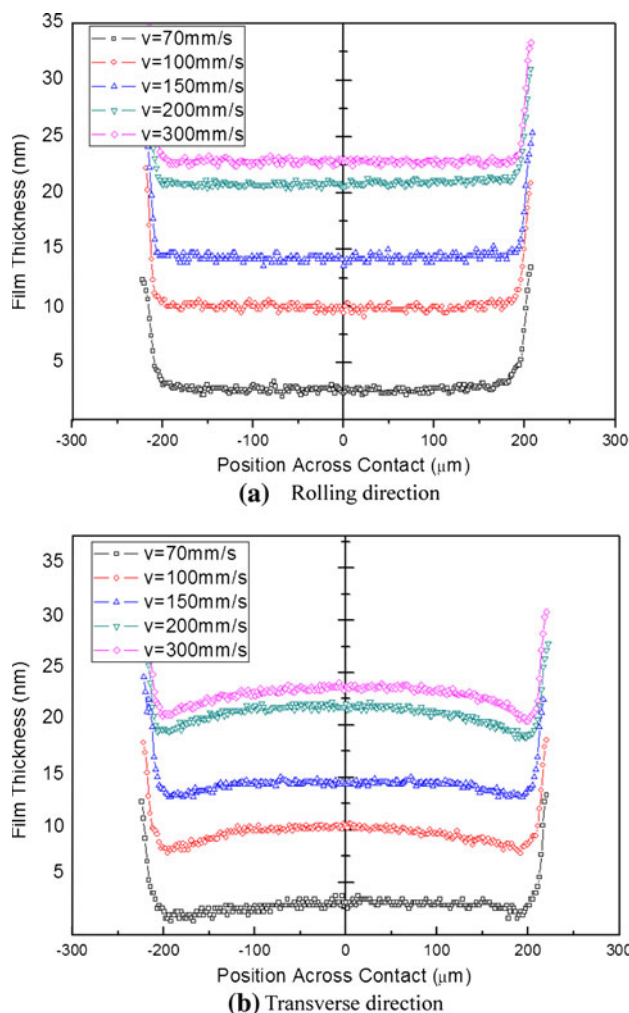


Fig. 10 Film thickness profiles for PAO 2 at 3 GPa

### 3.4 Results of Film Thickness Profiles

In addition to the relationship between film thickness and pressure or contact pressure, some previous studies [9, 19] have revealed that film thickness profiles also changed with both rolling speed and applied pressure. In this study, some results of film thickness profiles are also analyzed to show how the profiles are influenced at various conditions. Figures 10, 11, 12, 13, 14 and 15 show profiles of film thickness of PAO 2 and silicone oil 300. The profiles are taken in both the rolling and transverse directions at different speeds and contact pressures.

#### 3.4.1 PAO 2

The profiles of film thickness for PAO 2 at pressure of 3GPa are presented in Fig. 10. It can be seen that the profiles taken in rolling direction are similar for five different rolling speeds. In transverse direction, the difference

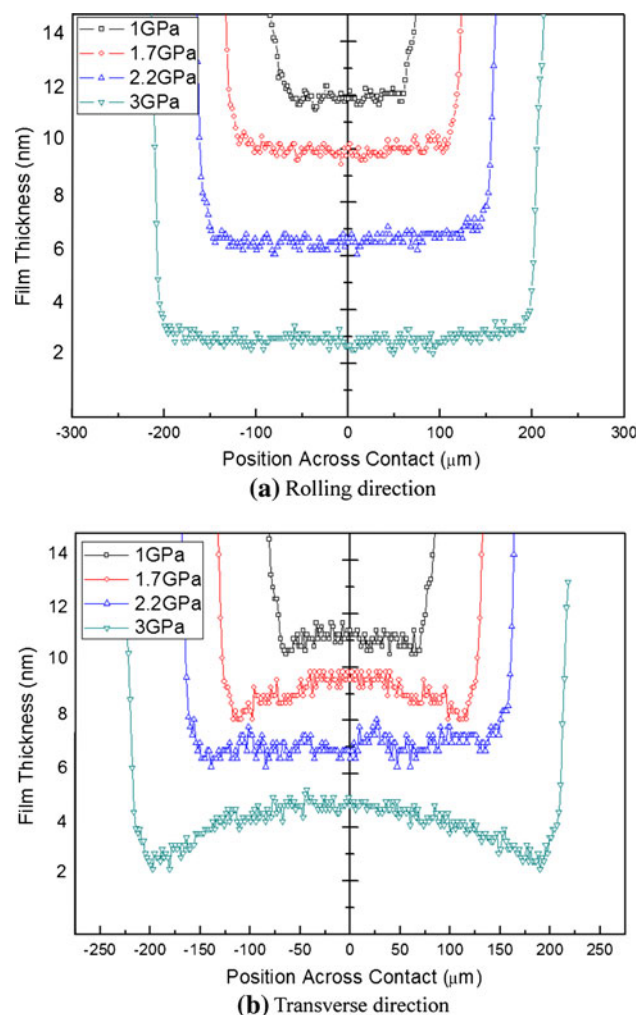


**Fig. 11** Film thickness profiles for PAO 2 at 100 mm/s

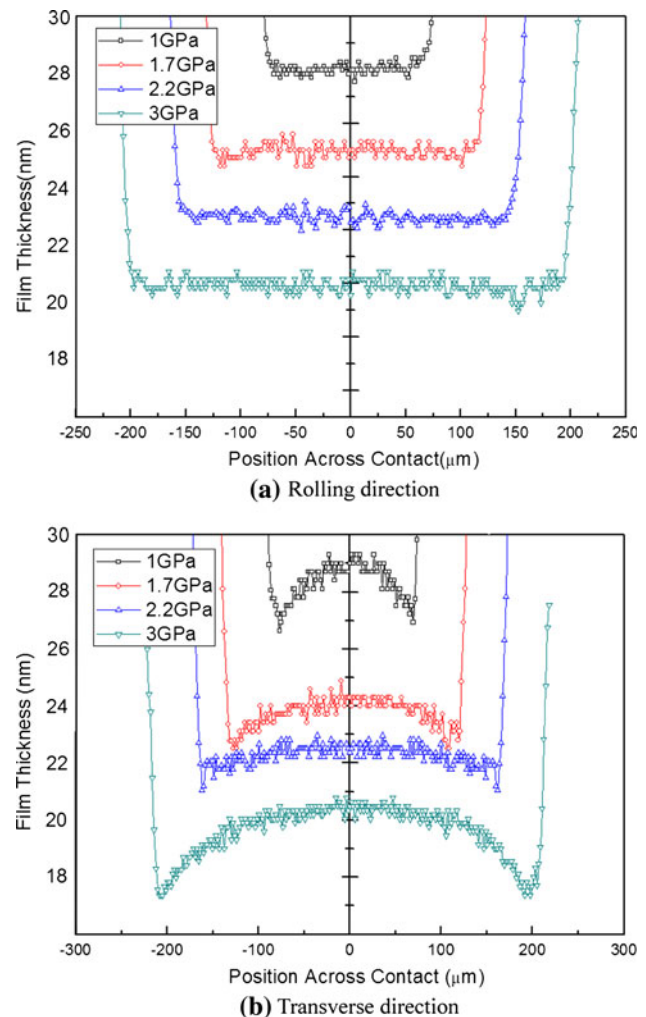


**Fig. 12** Film thickness profiles for PAO 2 at 300 mm/s

between central film thickness and minimum thickness gradually enlarges as the rolling speed rises. The profiles get more and more bow shaped during the same process.

The impact of contact pressure on film thickness profiles is emphasized in Figs. 11 and 12. There is little change of profiles with loads in rolling direction at speed of 100 and 300 mm/s. However, it should be noted that the central parts of profiles become smoother with increasing contact pressures.

#### 3.4.2 Silicone oil 300

Figure 13 shows the measured profiles of silicone oil 300 at 3 GPa for different speeds. The profiles change little in rolling speed direction, and with the increasing speed, the profiles show a more bow-shaped appearance in transverse direction which is similar to what is observed in PAO 2.

Some interesting properties are revealed in Figs. 14 and 15. When speed is low, the effect of pressure on profiles is

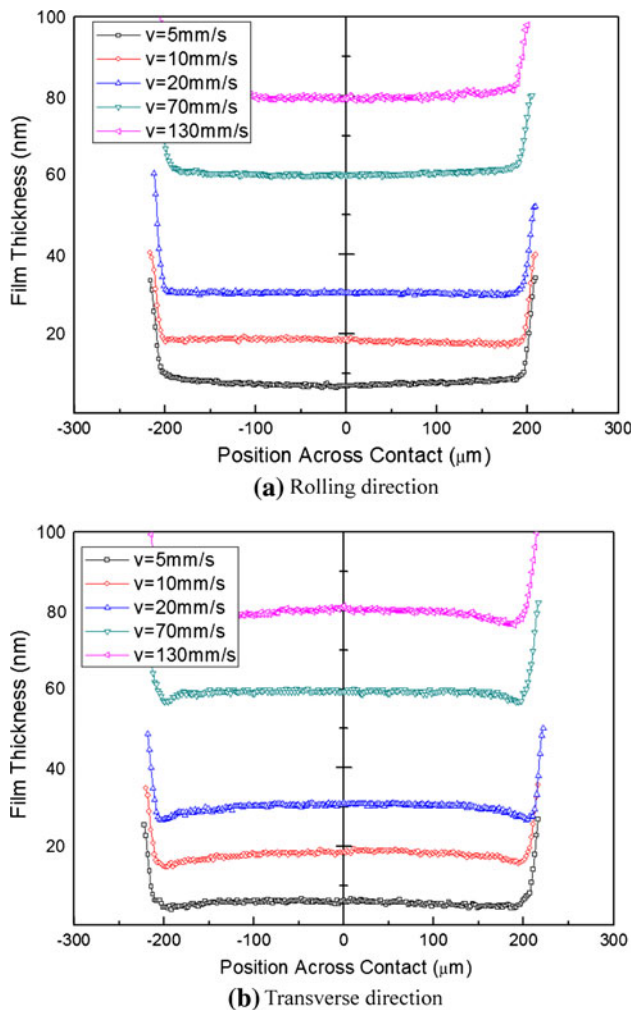


**Fig. 13** Film thickness profiles for silicone oil 300 at 3 GPa

not conspicuous as shown in Fig. 14. However, when speed reaches 120 mm/s, the influence of pressure is notable. First, in rolling direction, obvious outlet constriction can be detected. The outlet constriction rapidly decreases as more pressure is applied. At 1.7 and 2.2 GPa, a slight outlet constriction can be seen, but at high pressure up to 3 GPa, it totally disappears. Second, the profiles in transverse direction progressively platen with increasing pressure. The difference between the central film thickness and minimum film thickness reduces greatly.

The measured results of the film thickness profiles for silicone oil 300 agree excellently with the acquired interference image in transverse direction. In this direction, when contact pressure reaches 3 GPa, the two sides of film thickness profiles decrease with increasing rolling speed. Accordingly, it can be seen in Fig. 4b that central part becomes brighter than the two sides, when speed gradually rises. At the condition that the speed is stable with varying applied pressure, at low speeds, the difference between

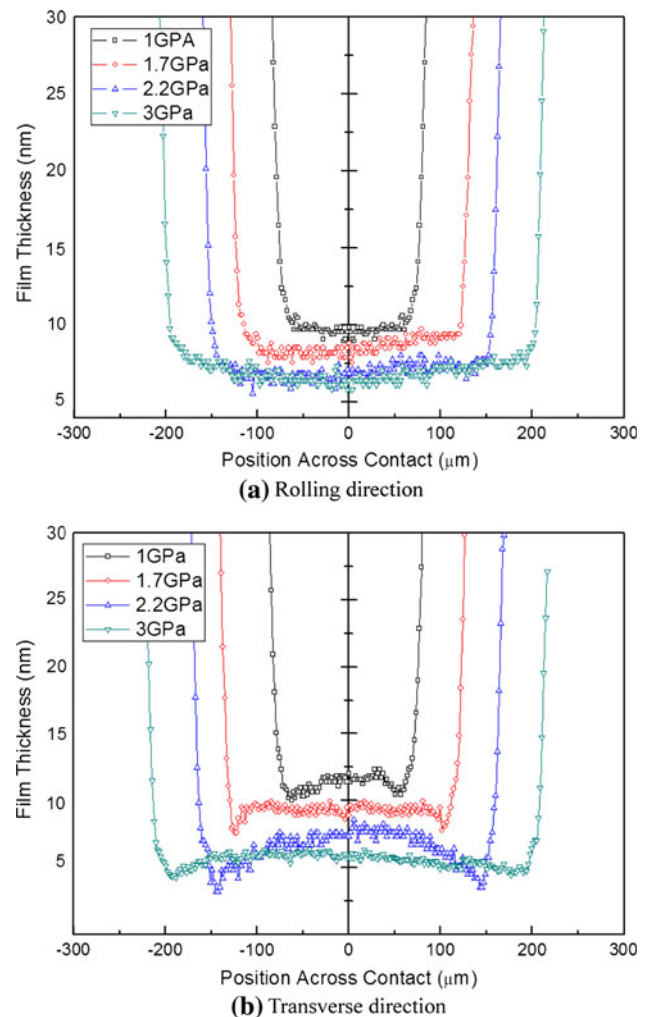


**Fig. 14** Film thickness profiles for silicone oil 300 at 5 mm/s

minimum film thickness and central film thickness is about 2–3 nm at the most, and the brightness of contact areas looks the same while pressure rises from 1 to 3 GPa. At high speed, however, the phenomenon is different. The difference between minimum and central film thickness is about 10 nm at 1 GPa, and 1–2 nm at 3 GPa. Therefore, in Fig. 4b, at 1 GPa and 160 mm/s, the central part is obviously brighter than the two sides. However, when contact pressure increases, the brightness contrast between central part and the sides reduces.

#### 4 Conclusions

A new film thickness measuring instrument is used to detect central film thicknesses of a series of lubricants at high contact pressure up to 3 GPa. Experimental results indicate that viscosity has different effects on the speed

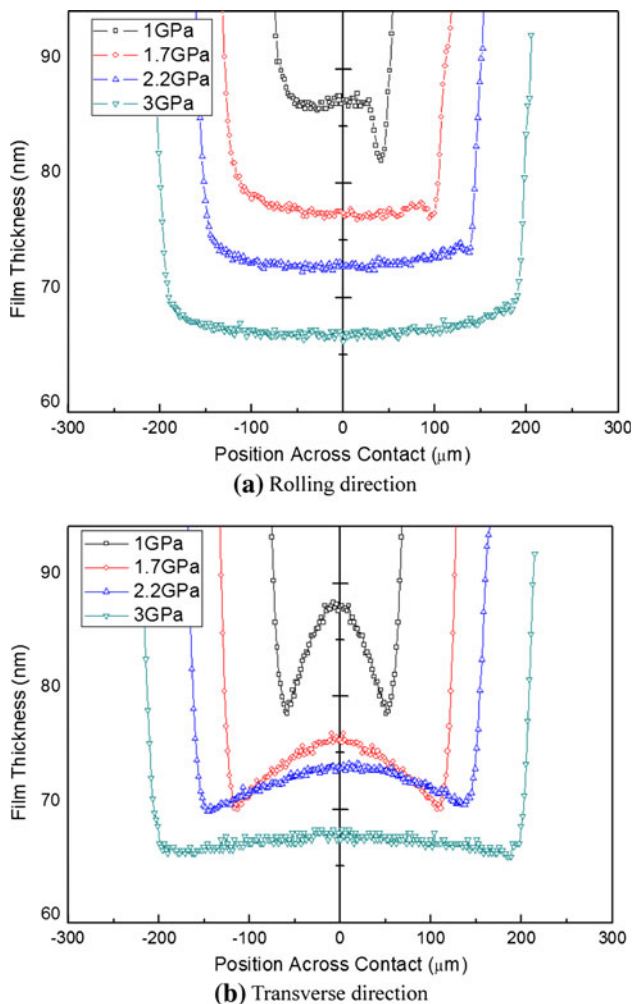


**Fig. 15** Film thickness profiles for silicone oil 300 at 120 mm/s

indexes of PAO and silicone oil. For PAO, speed index gradually reduces with increasing viscosity at both high and low rolling speed zones. For silicone oils, speed index changes little with viscosity in EHL. However, there is slight tendency of speed index to reduce with viscosity at low speed zone. The observed phenomenon is attributed to different fluidities and molecular structures of these base oils.

A comparison of experimental central film thickness with computational work has been made, and the results show that at high pressure conditions, the relationship between load and film thickness usually go against the prediction given by Hamrock and Dowson. The slope of the fitting lines can be either higher or lower than the predicted value based on the experimental results. Different compressibility of those lubricants is responsible for this behavior. Better compressibility indicates higher absolute value of slope of fitting line.

In addition, the results show that when higher pressure is applied, the profiles of film thickness become more and

more flat while the rolling speed does little to change the shape of profiles.

The results of this study reveal the lubrication properties of base oil of PAO and silicone oil at high contact pressure up to 3 GPa. What is more important, the behavior of commercial lubricants whose main components are those base oils can be concluded from this experimental result.

**Acknowledgments** The study is financially supported by the International Science & Technology Cooperation Project, and the National Key Basic Research Program of China (2007CB607604 and 2009CB724404). The authors are grateful to the NSK Ltd. for providing them with the high precision steel balls.

## References

1. Dowson, D., Higginson, G.R.: A numerical solution to the elasto-hydrodynamic problem. *J. Mech. Eng. Sci.* **1**, 6–15 (1959)
2. Hamrock, B.J., Dowson, D.: Isothermal elastohydrodynamic lubrication of point contacts. Part III—Fully flooded results. *J. Lubr. Technol.* **99**, 264–276 (1977)
3. Hardy, W.B., Doubleday, I.: Boundary lubrication—the paraffin series. *Proc. R. Soc. Lond. A.* **100**, 550–574 (1922)
4. Bowden, F.P., Tabor, D.: *The Friction and Lubrication of Solids*. Oxford University Press, Oxford (1954)
5. Adamson, A.W.: *The Physical Chemistry of Surfaces*, 3rd edn. Wiley, New York (1976)
6. Kingsbury, E.P.: Some aspects of the thermal of a boundary lubrication. *J. Appl. Phys.* **29**(6), 888–891 (1958)
7. Sharma, J.P., Cameron, A.: Surface-roughness and load in boundary lubrication. *Tribol. Trans.* **16**(4), 258–266 (1973)
8. Homola, A.M., Israelachvili, J.N., McGuiggan, P.M., Gee, M.L.: Fundamental experimental studies in tribology: the transition from ‘interfacial’ friction of undamaged molecularly smooth surfaces to ‘normal’ friction with wear. *Wear* **136**, 65–83 (1990)
9. Luo, J.B., Wen, S.Z., Huang, P.: Thin film lubrication Part 1: study on the transition between EHL and thin film lubrication using a relative optical interference intensity technique. *Wear* **194**, 107–115 (1996)
10. Patir, N., Cheng, H.S.: An average flow model for model for determining effect of three-dimensional roughness on partial hydrodynamic lubrication. *J. Lubr. Technol.* **100**, 12–17 (1978)
11. Wang, Q., Zhu, D.: Virtual texturing: modeling the performance of lubricated contacts of engineered surfaces. *Tribol. Trans.* **127**, 722–728 (2005)
12. Huang, P., Wen, S.Z.: Study on oil film and pressure distribution of micro-EHL. *Trans. ASME J. Tribol.* **114**, 42–46 (1992)
13. Lane, T.B., Hughes, J.R.: A study of the oil film formation in gears by electrical resistance measurements. *Br. J. Appl. Phys* **3**, 315 (1952)
14. Gohar, R., Cameron, A.: Optical measurement of oil film thickness under elastohydrodynamic lubrication. *Nature* **200**, 458 (1963)
15. Hartl, M., Krupka, I., Poliscuk, R., Liska, M.: Thin film colorimetric interferometry. *Tribol. Trans.* **44**(2), 270–276 (2001)
16. Glovnea, R.P., Forrest, A.K., Olver, A.V., Spikes, H.A.: Measurement of sub-nanometer lubricant films using ultra-thin film interferometry. *Tribol. Lett.* **15**(3), 217–230 (2003)
17. Zhu, D.: Elastohydrodynamic lubrication in extended parameter ranges—part 1: speed effect. *Tribol. Trans.* **45**, 540–548 (2002)
18. Zhu, D.: Elastohydrodynamic lubrication in extended parameter ranges—part 2: load effect. *Tribol. Trans.* **45**, 549–555 (2002)

19. Smeeth, M., Spikes, H.A.: Central and minimum elastohydrodynamic film thickness at high pressure. *Tribol. Trans.* **119**, 291–296 (1997)
20. Krupka, I., Hartl, M., Liska, M.: Thin lubricating films behavior at very high contact pressure. *Tribol. Int.* **39**, 1726–1731 (2006)
21. Ma, L., Zhang, C.: Discussion on the technique of relative optical interference intensity for the measurement of lubricant film thickness. *Tribol. Lett.* **36**, 239–245 (2009)
22. Vendam, K., Limsuwan, P.: Piezo- and elasto-optic properties of liquids under high pressures. II. Refractive index vs density. *J. Chem. Phys.* **69**, 4772–4778 (1978)
23. Glasstone, S.: *Textbook of Physical Chemistry*. Van Nostrand, New York (1946)
24. Dowson, D., Higginson, G.R.: *Elastohydrodynamic Lubrication*. Pergamon Press, Oxford (1966)